Pleiotrophin overexpression regulates amphetamine-induced reward and striatal dopaminergic denervation without changing the expression of dopamine D1 and D2 receptors: Implications for neuroinflammation

Marta Vicente-Rodríguez[†], Loreto Rojo Gonzalez[‡], Esther Gramage[†], Rosalía Fernández-Calle[†], Ying Chen[T], Carmen Pérez-García[†], Marcel Ferrer-Alcón[‡], María Uribarri[‡], Alexis Bailey[‡], Gonzalo Herradón[†,*]

[†] Pharmacology lab, Department of Pharmaceutical and Health Sciences. Facultad de Farmacia. Universidad CEU San Pablo, Madrid, Spain.

[T] Institute of Psychiatry, Psychology and Neuroscience, Division of Academic Psychiatry London, Kings College London, London, UK.

[‡] Department of Biochemistry & Physiology, Faculty of Health & Medical Sciences, University of Surrey, Guildford, UK.

Institute of Medical and Biomedical Education, St George's University of London, London SW17 0RE.

[‡] BRAINco Biopharma, S.L., Bizkaia Technology Park, Spain.

*Corresponding author:
Gonzalo Herradón, PhD
Lab. Pharmacology
Faculty of Pharmacy
Universidad CEU San Pablo
Urb. Montepríncipe
28668 Boadilla del Monte, Madrid, Spain.
Tel: 34-91-3724700 (Ext. 4840)
Fax: 34-91-3510475
e-mail: herradon@ceu.es

ABSTRACT

It was previously shown that mice with genetic deletion of the neurotrophic factor pleiotrophin (PTN-/-) show enhanced amphetamine neurotoxicity and impair extinction of amphetamine conditioned place preference (CPP), suggesting a modulatory role of PTN in amphetamine neurotoxicity and reward. We have now studied the effects of amphetamine (10 mg/kg, 4 times, every 2h) in the striatum of mice with transgenic PTN overexpression (PTN-Tg) in the brain and in wild type (WT) mice. Amphetamine caused an enhanced loss of striatal dopaminergic terminals, together with a highly significant aggravation of amphetamine-induced increase in the number of GFAP-positive astrocytes, in the striatum of PTN-Tg mice compared to WT mice. Given the known contribution of D1 and D2 dopamine receptors to the neurotoxic effects of amphetamine, we also performed quantitative receptor autoradiography of both receptors in the brains of PTN-Tg and WT mice. D1 and D2 receptors binding in the striatum and other regions of interest was not altered by genotype or treatment. Finally, we found that amphetamine CPP was significantly reduced in PTN-Tg mice. The data demonstrate that PTN overexpression in the brain blocks the conditioning effects of amphetamine and enhances the characteristic striatal dopaminergic denervation caused by this drug. These results indicate for the first time deleterious effects of PTN in vivo by mechanisms that are probably independent of changes in the expression of D1 and D2 dopamine receptors. The data also suggest that PTN-induced neuroinflammation could be involved in the enhanced neurotoxic effects of amphetamine in the striatum of PTN-Tg mice.

Keywords: Pleiotrophin, midkine, astrogliosis, inflammation, methamphetamine, reward.

1. INTRODUCTION

According to the European Monitoring Centre for Drugs and Drug Addiction, it is estimated that more than 2% of young people (15–34) used amphetamines in 2010 in different European countries including Czech Republic (3.2%), Denmark (3.1%), and the United Kingdom (2.3%). Ever in lifetime use of amphetamines among young people in those countries varies considerably, with levels of 30–70%. Despite widespread use of amphetamine-type stimulants, the long-term medical consequences of these drugs abuse and dependence have not been addressed until recently. During the past two decades, preclinical studies have demonstrated that this type of psychostimulants damages dopaminergic neurons, causing striatal dopaminergic denervation and dopaminergic cell death in the substantia nigra among other effects (Moratalla et al., 2015). However, clinical correlation was not studied until Callaghan and colleagues (2012) probed a ~77% increased risk of Parkinson's disease (PD) in amphetamine-type drug abusers (Callaghan et al., 2012). Similarly, a recent report indicates a 3-fold increased risk of PD in these drugs users (Curtin et al., 2015). Existence of genetic factors underlying individual vulnerability to the rewarding effects of amphetamine and dopaminergic neurotoxicity after consumption of this type of psychostimulants is known. Uncovering those genetic factors is not only clinically relevant but will also help to develop new therapeutic strategies for substance use disorders.

Pleiotrophin (PTN) is a neurotrophic factor known to play a role in amphetamine-induced neurotoxicity (Alguacil and Herradon, 2015). A single amphetamine administration causes a significant upregulation of PTN mRNA levels in the rat brain (Le

Greves, 2005) suggesting that PTN takes part in a modulatory mechanism against the effects of amphetamine in the brain. Accordingly, extinction of amphetamine-induced conditioned place preference (CPP) is impaired in PTN genetically deficient (PTN-/-) mice (Gramage et al., 2010a). Furthermore, a periadolescent amphetamine treatment was found to produce transient cognitive deficits only in PTN-/- mice, not in wild type (WT) mice (Gramage et al., 2013a). Interestingly, amphetamine-induced neurotoxic effects in the nigrostriatal pathway are enhanced in PTN-/- mice compared to WT mice (Gramage et al., 2010b; Soto-Montenegro et al., 2015). Also, it has to be noted that amphetamine-induced increase of GFAP-positive astrocytes, a hallmark of the neuroinflammation induced by this type of psychostimulants, was slightly increased in the striatum of PTN-/- mice (Gramage et al., 2010a). Overall, the data clearly suggest a modulatory role of PTN on amphetamine effects (Herradon and Perez-Garcia, 2014). However, the knockout mouse models, although invaluable as screening tools in research, have intrinsic limitations including ubiquitous absence of the targeted gene and possible developmentally-related mechanisms of compensation. To overcome these limitations, we have now studied the rewarding and neurotoxic effects of amphetamine in mice with transgenic neuronal PTN overexpression in the brain (PTN-Tg mice). In addition, it is interesting to note that overstimulation of dopamine D1 (D1R) and D2 receptors (D2R) significantly contributes to the neurotoxic effects of amphetamine (Moratalla et al., 2015). Furthermore, dopamine is a crucial transmitter in the neuroimmune network (Kustrimovic et al., 2014) and D2R is identified as an important component controlling innate immunity and inflammatory response in central nervous system (Shao et al., 2013). To test the possibility that differences in these receptors could underlie the different genotypic susceptibility to the neurotoxic and

neuroinflammatory effects of amphetamine, we carried out quantitative receptor autoradiography of D1, D2 receptors in the brains of PTN-Tg and WT mice.

2. EXPERIMENTAL PROCEDURES

2.1. Animals

PTN-Tg mice on a C57BL/6J background were generated by pronuclear injection as recently described (Ferrer-Alcón et al., 2012; Vicente-Rodriguez et al., 2014a). The acceptor vector used was pTSC-a2 and contained the regulatory regions responsible for tissue specific expression of Thy-1 gene, which drives neuron-specific expression of transgenes (Aigner et al., 1995; Caroni, 1997). PTN specific overexpression in different brain areas, including a 20% increase of PTN protein levels in striatum, was established by quantitative Real Time-Polymerase Chain Reaction (qRT-PCR), in situ hybridization, and by Western blot (Ferrer-Alcón et al., 2012; Vicente-Rodriguez et al., 2015; 2014b). Relevant to the behavioral study presented here, there were no differences in motor activity and exploration between both genotypes at baseline (Ferrer-Alcón et al., 2012).

We used male PTN-Tg and WT animals of 9-10 weeks (20-25 g). Mice were housed under controlled environmental conditions (22±1 ºC and a 12-h light/12-h dark cycle) with free access to food and water.

All the animals used in this study were maintained in accordance with European Union Laboratory Animal Care Rules (86/609/ECC directive) and the protocols were approved by the Animal Research Committee of USP-CEU.

2.2. Amphetamine treatment.

PTN-Tg and WT mice received 4 injections (i.p.) of amphetamine (10 mg/kg) or saline (control, 10 ml/kg), allowing between injections a 2 hour interval. This regimen of administrations of amphetamine was previously used to dissect differences between WT

and PTN-/- mice (Gramage et al., 2010a,b) and is known to cause significant damage to striatal dopaminergic terminals (Krasnova et al., 2001) and astrocytosis (Krasnova et al., 2005), a neuroinflammatory hallmark in the striatum that has been suggested to underlie the cognitive deficits, depression, and parkinsonism reported in amphetamine-type drugs addicts (Krasnova et al., 2016). Four days after the animals received the first administration of amphetamine or saline (control), mice were euthanized differently for immunohistochemistry and autoradiography studies.

2.3. Immunohistochemistry studies.

Mice were transcardially perfused with 4% p-formaldehyde and brains were removed and conserved in p-formaldehyde for 24 h and transferred to a 30% sucrose solution containing 0.02% sodium azide for storage at 4ºC. The brains were cut at a thickness of 30 µm using a vibratome (Leica, Wetzlar, Germany). Immunostaining was performed in one slice per 180 µm from bregma 1.54 mm to bregma 0.10 mm. Striatal free-floating sections were processed as previously described (Gramage et al., 2010a,b). In order to study astrogliosis or dopaminergic terminals, sections were incubated overnight at 4ºC with anti-GFAP antibodies (1:1000) (n = 4/group) or anti-TH antibodies (1:1000) (n = 6-7/group), respectively. Both antibodies were purchased from Millipore (Madrid, Spain). The sections were then rinsed in PBS three times for 10 min and incubated for 30 minutes with the biotinylated secondary antibodies in PBS at room temperature. The avidin–biotin reaction was performed using a Vectastain Elite ABC peroxidase kit following the protocol suggested by the manufacturer. The immunoreactivity was visualized using 0.06% diaminobenzidine and 0.03% H_2O_2 diluted in PBS. The sections were mounted on gelatin/chrome alume-coated slides, air-dried overnight, dehydrated through graded

ethanols, cleared in xylene, and coverslipped with DPX medium. Photomicrographs were captured with a digital camera coupled to an optical microscope (DMLS, Leica, Solms, Germany).

Image analysis was performed in the three most central slices of each animal. GFAP-positive astrocytes were counted in 325 x 435 µm standardized areas and TH-immunostaining density was analyzed in 230 ×140 µm areas, both located in the medial striatum (Gramage et al., 2010a,b).

The counting of GFAP-positive cells was accomplished with the help of the software Scion Image 4.02 (Scion Corporation, Frederick, MD, USA). As previously performed (Gramage et al., 2010b), cell counts were made in standardized areas (325 x 435 µm) obtaining the mean from three sections per animal. Striatal TH-positive fiber staining was assessed by optical density (OD) measurements using Image-Pro Plus software (Version 3.0.1; Media Cybernetics, Silver Spring, MD). For each animal, the nonspecific background correction in each section was done by subtracting the OD value of the corpus callosum from the striatal OD value obtained from the same section.

2.4. D1, D2 dopamine receptor and DAT autoradiography

Different cohorts of mice (n = 5-6/group) were sacrificed 4 days after the last injection of saline or amphetamine. The brains were immediately removed, quickly frozen in isopentane (-35ºC) and stored at -80ºC until sectioning. Quantitative autoradiography was performed as detailed previously for D1, D2 dopamine receptor binding and DAT binding (Bailey et al., 2008) using general procedures of Kitchen et al. (1997). Adjacent 20-µm brain coronal sections were cut at an interval of 300 µm for the determination of total and non-specific binding (NSB) of [^{3}H]SCH-23390 (containing 1 µM mianserin),

[^{3}H]raclopride and [^{3}H]mazindol (containing 0.3 μM desipramine) to D1R, D2R and DAT, respectively. Ligand concentrations were 3-4 x Kd, with all ligands used at a concentration of 4 nM. This sub-saturation concentration of radioligand was deliberately chosen in order to maximize the detection of binding differences if present. For instance, following this rationale we previously showed a clear downregulation of striatal [3H]raclopride (4nM) receptors in rats treated with chronic escalating dose "binge" cocaine administration paradigm but not following chronic steady dose "binge" cocaine administration (Bailey et al., 2008). NSB was defined in the presence of cis-flupentixol (10 μM), sulpiride (10 μM) or unlabeled mazindol (10 μM) for [^{3}H]SCH-23390, [^{3}H]raclopride and [^{3}H]mazindol binding, respectively. Following incubation binding for a period of 90 min or 60 min at room temperature or 45 min at 4ºC for D1R, D2R and DAT, respectively, and washing in ice-cold buffer (6 x 1 min for D1R and D2R binding and 2 x 1 min for DAT binding), the slides were apposed to MR film (Eastman Kodak Co., Rochester, NY, USA) in X-ray cassettes together with a set of tritium standards ([^{3}H]Microscale™, Amersham, UK) for 6 weeks. Sections were processed together in a paired protocol. Films were developed using 50% Kodak D19 developer. Quantitative analysis of brain receptors was performed as detailed previously (Kitchen et al., 1997; Lena et al., 2004). Using a MCID image analyser (Image Research, Canada), brain structures were identified using the mouse brain atlas of Franklin & Paxinos (1997). Brain images were analyzed using left and right hemispheres to allow duplication of results. The cortical and olfactory tubercle structures were analyzed by sampling five to eight times with a box size 15 × 15 mm^2 in a box tool. All other regions were analyzed by freehand drawing tools.

2.5. Conditioned Place Preference (CPP)

A biased apparatus was used as previously described (Vicente-Rodriguez et al., 2014a). One compartment had black floor and walls, and the other had black floor and white walls. The phases of CPP included preconditioning (day 1), conditioning (days 2-4) and testing (day 5). During preconditioning, mice were free to explore the two compartments for a 30-min period; their behavior was monitored by a videotracking system (San Diego, California, USA) to calculate the time spent in each compartment. Mice were counterbalanced such that half the animals started in one chamber and half started in the other. The compartment with white walls was the non-preferred compartment in a similar manner by both genotypes (30 - 40% stay of total time in the preconditioning phase). This `biased` apparatus and subject assignment, in which mice are paired with the drug in the non-preferred compartment, was previously used to study genotypic differences in amphetamine- and cocaine-induced CPP (Gramage et al., 2013b; Gramage et al., 2010b). The conditioning phase consisted of double conditioning sessions (Gramage et al., 2013b). The first one involved a morning session starting at 8 am. All animals received a single injection of saline i.p. (10 ml/kg) and were confined to the initially preferred compartment for 30 min. In the evening session, starting at 3 pm, the animals were injected (i.p.) with 3.0 mg/kg amphetamine (n = 10-15/group), or 10 ml/kg saline (n = 5-7/group) as a conditioning control, and confined to the initially non-preferred compartment for 30 min. The procedure used in days 3 and 4 was the same but the order of the treatments (morning/evening) was changed to avoid the influence of circadian variability. In the testing phase, mice received a drug-free, 30-min preference test. The time-spent in the non-preferred (drug-paired) compartment was calculated in all cases. The increase in the time-spent in the drug-paired compartment in day 5 compared to day 1 (preference score) was considered as indicative of the degree of conditioning induced by amphetamine.

2.6. Statistics

All data were expressed as the mean ± SEM and analyzed using Prism software (GraphPad, La Jolla, CA, USA). Data obtained from image analysis of striatal immunostaining and autoradiography were analyzed using two-way ANOVA. Relevant differences were analyzed pair-wise by post-hoc comparisons with Bonferroni's post-hoc tests, considering genotype (PTN-Tg, WT) and treatment (saline, amphetamine) as between-subjects factors. Amphetamine preference scores from CPP were confirmed to follow a normal distribution with Kolmogorov-Smirnov, D'Agostino and Pearson Omnibus and Shapiro-Wilk normality tests, so they were analyzed using a Student's t-test. $P < 0.05$ was considered as statistically significant.

3. RESULTS

3.1. Enhanced amphetamine-induced loss of dopaminergic terminals in the striatum of PTN-Tg mice.

Since one of the most relevant consequences of amphetamine administration is the loss of dopaminergic terminals in the striatum (Bowyer et al., 1998), we analyzed TH expression by immunohistochemistry and DAT expression by autoradiography in the Caudate Putamen (CPu) of PTN-Tg and WT mice treated with either amphetamine or saline (control). Two-way ANOVA revealed a significant effect of the genotype ($F(1,21) = 9.148$; $P = 0.0064$), of the treatment ($F(1,21) = 44.66$; $P < 0.0001$) and a significant interaction between genotype and treatment ($F(1,21) = 5.749$; $P < 0.0259$) on striatal TH expression. Amphetamine caused a ~40 % depletion of TH contents in the CPu of WT mice compared with saline-treated WT mice (Fig. 1). We detected a significantly greater decrease of TH levels in the CPu of amphetamine-treated PTN-Tg mice compared to WT mice (Fig. 1). However, we did not find significant differences in the levels of TH in the striatum of saline-treated PTN-Tg and WT mice (Fig. 1).

In order to discard the possibility that genotypic differences in amphetamine-induced TH loss could be related to differences in this enzyme's transcription and non-necessarily to an enhanced loss of dopaminergic terminals, we tested DAT expression by autoradiography in the CPu (Fig. 2). As expected, amphetamine showed a significant impact in striatal DAT contents ($F(1,20) = 28.54$; $P < 0.0001$). Amphetamine tended to produce a greater decrease of DAT levels in the CPu of PTN-Tg mice (Fig. 2B). Considering the medial CPu, DAT levels were significantly reduced by amphetamine

treatment only in PTN-Tg mice (Fig. 2C), whereas reduction of DAT levels was not statistically different in the lateral CPu of both genotypes (Fig. 2D).

3.2. Enhanced amphetamine-induced increase of GFAP-positive astrocytes in the striatum of PTN-Tg mice.

In these experiments, very few GFAP-positive astrocytes were observed in the striata of saline-treated mice (Fig. 3A). These cells were characterized by small cell bodies as well as very fine and short processes. In contrast, after amphetamine administrations, GFAP-positive astrocytes developed large cell bodies as well as long and extensive processes (Fig. 3A). In the case of amphetamine-treated PTN-Tg mice, astrocytes developed larger densely stained cell bodies as well as longer processes compared with WT mice (Fig. 3A). In addition, two-way ANOVA revealed a significant effect of the genotype ($F(1,12) = 24.08$; $P = 0.0004$), of the treatment ($F(1,12) = 62.93$; $P < 0.0001$) and a significant interaction between genotype and treatment ($F(1,12) = 20.48$; $P < 0.001$) on the number of GFAP+ cells/mm^2 in the striatum. The number of GFAP+ cells in amphetamine-treated mice increased in both genotypes when compared to the saline-treated groups (Fig. 3B). However, a highly significant increase in the number of GFAP-positive astrocytes in the striata of PTN-Tg mice compared to WT mice was found (Fig. 3B).

3.3. D1, D2 binding in the brains of WT and PTN-Tg mice.

No significant differences in D1, D2 receptors binding were observed in the CPu of PTN-Tg and WT mice (Figs. 4, 5). When medial and lateral CPu were analyzed separately, D1R and D2R binding was found to be similar in both genotypes (Figs. 4, 5). In addition,

no significant genotype or treatment effect was detected in D1 binding (table 1) and in D2 binding (table 2) in any of the regions analyzed.

3.4. Decreased amphetamine-induced conditioned place preference in PTN-Tg mice.

To test the possibility that PTN could modulate amphetamine rewarding effects, we performed conditioning studies. We used a medium dose of amphetamine (3.0 g/kg, i.p.) known to induce CPP in this mouse strain (Gramage et al., 2010a; Tzschentke, 2007). Thus, as expected, amphetamine caused a robust CPP in WT mice (Fig. 6). However, amphetamine place preference score was decreased by 65 percent in PTN-Tg mice (Fig. 6, [$t_{(22)}$=2.29, P=0.031]). As shown before with the same genotypes (Vicente-Rodriguez et al., 2014a), saline conditioning did not show significant changes on place preference compared to preconditioning values of both genotypes (data not shown). The data confirm an important role of PTN in the regulation of the rewarding effects of amphetamine.

4. DISCUSSION

In previous studies, it was shown that PTN-/- mice exhibit exacerbated amphetamine-induced dopaminergic damage in the nigrostriatal pathway (Gramage et al., 2010a; 2010b). Thus, we hypothesized a possible neuroprotective role of PTN in response to the neurotoxic effects of amphetamine. However, one has to be cautious in making conclusions from knockout mice assays as data collected in these mice are subjected to the inherent limitations of a constitutive knockout animal model. To evaluate the potential neuroprotective role of PTN against amphetamine-induced neurotoxicity, we have now studied the effects of this drug in the striatum of mice with transgenic overexpression of PTN in the brain. In support of this rationale, studies with parkinsonian toxins had previously shown that overexpression of PTN exerts neuroprotection in mouse models of PD (Gombash et al., 2012; 2014). Unexpectedly, we found that amphetamine-induced loss of striatal TH and DAT contents is increased in PTN-Tg mice, suggesting that dopaminergic denervation caused by amphetamine is facilitated by PTN overexpression. This apparent discrepancy in the data collected from amphetamine-treated PTN-/- and PTN-Tg mice may reflect the possibility of compensatory mechanisms triggered by the elimination of PTN during development in the PTN knockout mice. These compensatory mechanisms are not clear but could be related to the signaling pathways regulated by PTN. PTN binds Receptor Protein Tyrosine Phosphatase (RPTP) β/ζ (also known as PTPRZ1) and inactivate its intrinsic tyrosine phosphatase activity (Gramage and Herradon, 2011). As a result, PTN causes increases in the phosphorylation levels of substrates of RPTPβ/ζ known to be important for neuronal function (e.g. Fyn kinase and β-catenin) which, in turn, trigger other signaling pathways involved in different functions including mitogenic,

differentiation, survival and inflammation (Herradon and Perez-Garcia, 2014). Thus, it seems reasonable to hypothesize that some substrates of RPTPβ/ζ, or downstream factors in their signaling pathways, could be involved in compensatory developmental mechanisms in PTN-/- mice.

The neuroprotective effects of PTN against cocaine- and amphetamine-induced toxicity have been proven in vitro. PTN (3 μM) limits amphetamine- and cocaine-induced decrease in PC12 and NG108-15 cell viability (Gramage et al., 2008; Gramage et al., 2010a; 2010b). However, our results show that the net effect produced by PTN seems to differ in vivo, suggesting overall deleterious effects triggered by activation of PTN downstream pathways that could counteract its trophic actions on neurons. For instance, PTN induces the proliferation of immune cells and the expression of inflammatory cytokines including TNF-alpha, IL-1beta and IL-6 (Achour et al., 2001; 2008), suggesting a proinflammatory role of PTN. Previously, we showed a modest increase (~20%) of amphetamine-induced GFAP-positive astrocytes in PTN-/- mice (Gramage et al., 2010a). We now show a 13-fold upregulation of GFAP+ cells in the striatum of amphetamine-treated PTN-Tg mice. Since merely a few astrocytes were sparsely detected throughout the striatum of control mice and it is known that GFAP labeling of striatal astrocytes can be sparse compared with other astrocyte markers in naïve animals (Kalman and Hajos, 1989; Krasnova et al., 2005; Tong et al., 2014), our data should not be interpreted as changes to astrocyte density without further confirmation. Most likely, our data reflect a highly significant amphetamine-induced upregulation of GFAP protein concentrations in astrocytes. Although a limitation of the present study is that microglial response has not been assessed, it has to be noted that overexpression of GFAP is an indicator of reactive astrogliosis and neuroinflammation, important events in a wide variety of CNS disorders

and pathologies (Sofroniew and Vinters, 2010). Thus, the robust increase of GFAP-positive astrocytes in amphetamine-treated PTN-Tg mice suggests an enhanced neuroinflammation induced by amphetamine in the presence of higher levels of PTN. Indeed these findings clearly indicate that PTN is involved in the neuroinflammatory promoting effect of amphetamine. A proposed model for this is illustrated in Fig. 7. It is important to note that different drugs of abuse, including amphetamine and its derivatives, induce neuroinflammation (Coelho-Santos et al., 2012) and that exacerbated neuroinflammatory responses, including astrocytosis, have been linked to neurodegenerative processes and CNS injury in different models (Qin et al., 2007; Sanchez-Guajardo et al., 2013). Our current findings, together with the fact that amphetamine administration increases the levels of expression of PTN in the brain (Le Greves, 2005), suggest the possibility that PTN may be one of the mediators facilitating amphetamine-induced neuroinflammation and, as a result, neurotoxicity (Fig. 7).

The major cause of amphetamines neurotoxicity in the striatum is the dysregulation of dopamine and dopamine receptors (Ares-Santos et al., 2013). It has been shown that D1R antagonists protect against amphetamines-induced decreases in DAT binding in the striatum (Angulo et al., 2004) and inhibit the striatal denervation caused by these drugs (Xu et al., 2005). In a similar manner, inactivation of D2R prevents methamphetamine-induced reductions of striatal TH and DAT levels (Ares-Santos et al., 2013). Interestingly, the use of antagonists or genetic inactivation of D1R and D2R has been shown to reduce the enhanced striatal astrogliosis induced by amphetamines (Ares-Santos et al., 2013; Xu et al., 2005), suggesting that both receptors are also involved in the neuroinflammation caused by this type of drugs. However, our data demonstrate that D1R and D2R binding is not altered by amphetamine treatment and is similar in all the brain regions analyzed, including striatum,

of PTN-Tg and WT mice. The data clearly suggest that amphetamine-induced enhanced fibre loss and astrogliosis in the striatum of PTN-Tg mice is independent of D1R- and D2R-related mechanisms at least at the receptor expression level.

Finally, we also tested the rewarding effects of amphetamine in PTN-Tg and WT mice. We previously found that amphetamine induces place preference in both PTN knockout and WT mice in a similar manner (Gramage et al., 2010a). However, extinction of amphetamine-induced CPP was delayed in PTN-/- mice suggesting a possible role of PTN in amphetamine reward. In the present work, our results uncover that overexpression of PTN significantly blocks amphetamine-induced conditioned place preference, suggesting an important role of PTN in the limitation of the rewarding effects of amphetamine. Interestingly, it was recently shown that alcohol-induced CPP was completely absent in PTN-Tg mice (Vicente-Rodriguez et al., 2014a). Overall, the data suggest a hyporeactive rewarding system of PTN-Tg mice in response to different drugs of abuse that is not related to deficits in D1, D2 receptors expression levels.

In summary, the present study clarifies the role of PTN in amphetamine-induced neurotoxicity and reward. We demonstrate for the first time that brain overexpression of PTN blocks amphetamine-induced CPP. We also demonstrate that the net effect of brain overexpression of PTN is the enhancement of amphetamine-induced neurotoxic effects in the striatum despite previous evidences in PTN-/- mice pointing to an overall neuroprotective role of PTN in this context. In addition, the data demonstrate that increased amphetamine neurotoxicity in the striatum caused by overexpression of PTN is not related to changes in D1R and D2R expression. The data suggest that enhanced neuroinflammation

triggered by PTN overexpression could be involved in the greater striatal dopaminergic denervation caused by amphetamine in PTN-Tg mice.

Acknowledgements: This work has been supported by grants SAF2014-56671-R from Ministerio de Economía y Competitividad of Spain and USP-BS-APP03/2014 from Universidad CEU San Pablo and Banco de Santander to GH. M V-R and R F-C are supported by fellowships from Fundación Universitaria San Pablo CEU. M V-R was supported by a travel grant CEU-Banco de Santander in Biochemistry & Physiology Department, University of Surrey, Guildford (UK).

REFERENCES

Achour, A., Laaroubi, D., Caruelle, D., Barritault, D., Courty, J., 2001. The angiogenic factor heparin affin regulatory peptide (HARP) induces proliferation of human peripheral blood mononuclear cells. Cell Mol Biol (Noisy-le-grand) 47 Online Pub, OL73-77.

Achour, A., M'Bika J, P., Baudouin, F., Caruelle, D., Courty, J., 2008. Pleiotrophin induces expression of inflammatory cytokines in peripheral blood mononuclear cells. Biochimie 90, 1791-1795.

Aigner, L., Arber, S., Kapfhammer, J.P., Laux, T., Schneider, C., Botteri, F., Brenner, H.R., Caroni, P., 1995. Overexpression of the neural growth-associated protein GAP-43 induces nerve sprouting in the adult nervous system of transgenic mice. Cell 83, 269-278.

Alguacil, L.F., Herradon, G., 2015. Midkine and Pleiotrophin in the Treatment of Neurodegenerative Diseases and Drug Addiction. Recent Pat CNS Drug Discov 10, 28-33.

Angulo, J.A., Angulo, N., Yu, J., 2004. Antagonists of the neurokinin-1 or dopamine D1 receptors confer protection from methamphetamine on dopamine terminals of the mouse striatum. Ann N Y Acad Sci 1025, 171-180.

Ares-Santos, S., Granado, N., Moratalla, R., 2013. The role of dopamine receptors in the neurotoxicity of methamphetamine. J Intern Med 273, 437-453.

Bailey, A., Metaxas, A., Yoo, J.H., McGee, T., Kitchen, I., 2008. Decrease of D2 receptor binding but increase in D2-stimulated G-protein activation, dopamine transporter binding and behavioural sensitization in brains of mice treated with a chronic escalating dose 'binge' cocaine administration paradigm. Eur J Neurosci 28, 759-770.

Bowyer, J.F., Frame, L.T., Clausing, P., Nagamoto-Combs, K., Osterhout, C.A., Sterling, C.R., Tank, A.W., 1998. Long-term effects of amphetamine neurotoxicity on tyrosine hydroxylase mRNA and protein in aged rats. J Pharmacol Exp Ther 286, 1074-1085.

Callaghan, R.C., Cunningham, J.K., Sykes, J., Kish, S.J., 2012. Increased risk of Parkinson's disease in individuals hospitalized with conditions related to the use of methamphetamine or other amphetamine-type drugs. Drug Alcohol Depend 120, 35-40.

Caroni, P., 1997. Overexpression of growth-associated proteins in the neurons of adult transgenic mice. J Neurosci Methods 71, 3-9.

Coelho-Santos, V., Goncalves, J., Fontes-Ribeiro, C., Silva, A.P., 2012. Prevention of methamphetamine-induced microglial cell death by TNF-alpha and IL-6 through activation of the JAK-STAT pathway. J Neuroinflammation 9, 103.

Curtin, K., Fleckenstein, A.E., Robison, R.J., Crookston, M.J., Smith, K.R., Hanson, G.R., 2015. Methamphetamine/amphetamine abuse and risk of Parkinson's disease in Utah: a population-based assessment. Drug Alcohol Depend 146, 30-38.

Ferrer-Alcón, M., Uribarri, M., Díaz, A., Del Olmo, N., Valdizán, E.M., Gramage, E., Martín, M., Castro, E., Pérez-García, C., Mengod, G., Maldonado, R., Herradon, G., Pazos, A., Palacios, J.M., 2012. A new non-classical transgenic animal model of Depression Program No. 776.04/FF9 Neuroscience Meeting Planner. New Orleans, LA: Society for Neuroscience, 2012. Online.

Gombash, S.E., Lipton, J.W., Collier, T.J., Madhavan, L., Steece-Collier, K., Cole-Strauss, A., Terpstra, B.T., Spieles-Engemann, A.L., Daley, B.F., Wohlgenant, S.L., Thompson, V.B., Manfredsson, F.P., Mandel, R.J., Sortwell, C.E., 2012. Striatal pleiotrophin overexpression provides functional and morphological neuroprotection in the 6-hydroxydopamine model. Mol Ther 20, 544-554.

Gombash, S.E., Manfredsson, F.P., Mandel, R.J., Collier, T.J., Fischer, D.L., Kemp, C.J., Kuhn, N.M., Wohlgenant, S.L., Fleming, S.M., Sortwell, C.E., 2014. Neuroprotective potential of pleiotrophin overexpression in the striatonigral pathway compared with overexpression in both the striatonigral and nigrostriatal pathways. Gene Ther 21, 682-693.

Gramage, E., Alguacil, L.F., Herradon, G., 2008. Pleiotrophin prevents cocaine-induced toxicity in vitro. Eur J Pharmacol 595, 35-38.

Gramage, E., Del Olmo, N., Fole, A., Martin, Y.B., Herradon, G., 2013a. Periadolescent amphetamine treatment causes transient cognitive disruptions and long-term changes in hippocampal LTP depending on the endogenous expression of pleiotrophin. Addict Biol 18, 19-29.

Gramage, E., Herradon, G., 2011. Connecting Parkinson's disease and drug addiction: common players reveal unexpected disease connections and novel therapeutic approaches. Curr Pharm Des 17, 449-461.

Gramage, E., Perez-Garcia, C., Vicente-Rodriguez, M., Bollen, S., Rojo, L., Herradon, G., 2013b. Regulation of extinction of cocaine-induced place preference by midkine is related to a differential phosphorylation of peroxiredoxin 6 in dorsal striatum. Behav Brain Res 253, 223-231.

Gramage, E., Putelli, A., Polanco, M.J., Gonzalez-Martin, C., Ezquerra, L., Alguacil, L.F., Perez-Pinera, P., Deuel, T.F., Herradon, G., 2010a. The neurotrophic factor pleiotrophin modulates amphetamine-seeking behaviour and amphetamine-induced neurotoxic effects: evidence from pleiotrophin knockout mice. Addict Biol 15, 403-412.

Gramage, E., Rossi, L., Granado, N., Moratalla, R., Herradon, G., 2010b. Genetic inactivation of pleiotrophin triggers amphetamine-induced cell loss in the substantia nigra and enhances amphetamine neurotoxicity in the striatum. Neuroscience 170, 308-316.

Herradon, G., Perez-Garcia, C., 2014. Targeting midkine and pleiotrophin signaling pathways in addiction and neurodegenerative disorders: Recent progress and perspectives. Br J Pharmacol 171, 837-848.

Kalman, M., Hajos, F., 1989. Distribution of glial fibrillary acidic protein (GFAP)-immunoreactive astrocytes in the rat brain. Exp Brain Res 78, 147–163.

Kitchen, I., Slowe, S.J., Matthes, H.W., Kieffer, B., 1997. Quantitative autoradiographic mapping of mu-, delta- and kappa-opioid receptors in knockout mice lacking the mu-opioid receptor gene. Brain Res 778, 73-88.

Krasnova, I.N., Ladenheim, B., Jayanthi, S., Oyler, J., Moran, T.H., Huestis, M.A., Cadet, J.L., 2001. Amphetamine-induced toxicity in dopamine terminals in CD-1 and C57BL/6J mice: complex roles for oxygen-based species and temperature regulation. Neuroscience 107, 265-274.

Krasnova, I.N., Ladenheim, B., Cadet, J.L., 2005. Amphetamine induces apoptosis of medium spiny striatal projection neurons via the mitochondria-dependent pathway. FASEB J 19, 851-853.

Krasnova, I.N., Justinova, Z., Cadet, J.L. , 2016. Methamphetamine addiction: involvement of CREB and neuroinflammatory signaling pathways. Psychopharmacology, *in press*.

Kustrimovic, N., Rasini, E., Legnaro, M., Marino, F., Cosentino, M., 2014. Expression of dopaminergic receptors on human CD4+ T lymphocytes: flow cytometric analysis of naive and memory subsets and relevance for the neuroimmunology of neurodegenerative disease. J Neuroimmune Pharmacol 9, 302-312.

Le Greves, P., 2005. Pleiotrophin gene transcription in the rat nucleus accumbens is stimulated by an acute dose of amphetamine. Brain Res Bull 65, 529-532.

Lena, I., Matthes, H., Kieffer, B., Kitchen, I., 2004. Quantitative autoradiography of dopamine receptors in the brains of micro-opioid receptor knockout mice. Neurosci Lett 356, 220-224.

Moratalla, R., Khairnar, A., Simola, N., Granado, N., Garcia-Montes, J.R., Porceddu, P.F., Tizabi, Y., Costa, G., Morelli, M., 2015. Amphetamine-related drugs neurotoxicity in humans and in experimental animals: Main mechanisms. Prog Neurobiol.

Qin, L., Wu, X., Block, M.L., Liu, Y., Breese, G.R., Hong, J.S., Knapp, D.J., Crews, F.T., 2007. Systemic LPS causes chronic neuroinflammation and progressive neurodegeneration. Glia 55, 453-462.

Sanchez-Guajardo, V., Barnum, C.J., Tansey, M.G., Romero-Ramos, M., 2013. Neuroimmunological processes in Parkinson's disease and their relation to alpha-synuclein: microglia as the referee between neuronal processes and peripheral immunity. ASN Neuro 5, 113-139.

Shao, W., Zhang, S.Z., Tang, M., Zhang, X.H., Zhou, Z., Yin, Y.Q., Zhou, Q.B., Huang, Y.Y., Liu, Y.J., Wawrousek, E., Chen, T., Li, S.B., Xu, M., Zhou, J.N., Hu, G., Zhou, J.W., 2013. Suppression of neuroinflammation by astrocytic dopamine D2 receptors via alphaB-crystallin. Nature 494, 90-94.

Sofroniew, M.V., Vinters, H.V., 2010. Astrocytes: biology and pathology. Acta Neuropathol. 119, 7-35.

Soto-Montenegro, M.L., Vicente-Rodriguez, M., Perez-Garcia, C., Gramage, E., Desco, M., Herradon, G., 2015. Functional neuroimaging of amphetamine-induced striatal neurotoxicity in the pleiotrophin knockout mouse model. Neurosci Lett 591, 132-137.

Tong, X., Ao, Y., Faas, G.C., Nwaobi, S.E., Xu, J., Haustein, M.D., Anderson, M.A., Mody, I., Olsen, M.L., Sofroniew, M.V., Khakh, B.S., 2014. Astrocyte Kir4.1 ion channel deficits contribute to neuronal dysfunction in Huntington's disease model mice. Nat Neurosci. 17, 694-703.

Tzschentke, T.M., 2007. Measuring reward with the conditioned place preference (CPP) paradigm: update of the last decade. Addict Biol 12, 227-462.

Vicente-Rodriguez, M., Herradon, G., Ferrer-Alcon, M., Uribarri, M., Perez-Garcia, C., 2015. Chronic Cocaine Use Causes Changes in the Striatal Proteome Depending on the Endogenous Expression of Pleiotrophin. Chem Res Toxicol 28, 1443-1454.

Vicente-Rodriguez, M., Perez-Garcia, C., Ferrer-Alcon, M., Uribarri, M., Sanchez-Alonso, M.G., Ramos, M.P., Herradon, G., 2014a. Pleiotrophin differentially regulates the rewarding and sedative effects of ethanol. J Neurochem 131, 688-695.

Vicente-Rodriguez, M., Perez-Garcia, C., Haro, M., Ramos, M.P., Herradon, G., 2014b. Genetic inactivation of midkine modulates behavioural responses to ethanol possibly by enhancing GABA(A) receptor sensitivity to GABA(A) acting drugs. Behav Brain Res 274, 258-263.

Xu, Z.C., Ling, G., Sahr, R.N., Neal-Beliveau, B.S., 2005. Asymmetrical changes of dopamine receptors in the striatum after unilateral dopamine depletion. Brain Res 1038, 163-170.

FIGURE LEGENDS

Fig. 1. TH expression in striatum of PTN-Tg and WT mice after amphetamine administration. TH-immunostained striatal sections of mice treated with saline (Sal) or amphetamine (Amph) (n=6-7/group). (A) Photomicrographs illustrate that PTN overexpression increases amphetamine-induced TH loss. (B) Graph represents the optical density (OD) measures of TH-ir in the striatum. ** $p < 0.01$ vs. Sal. *** $p < 0.001$ vs. Sal. # $p < 0.05$ vs. WT-Amph. Scale bar = 300 μm.

Fig. 2. [^{3}H]mazindol binding in WT and PTN-Tg mice treated with amphetamine. (A) Representative autoradiograms of [^{3}H]mazindol binding to DAT in the brain sections of WT and PTN-Tg mice treated with saline (Sal) or amphetamine (Amph) (n=6/group). Representative autoradiograms of non-specific binding (NSB) was determined in the presence of 10 μM mazindol. The colour bar represents pseudo-color interpretation of black and white film images in fmol/mg tissue. (B) Quantitative autoradiography of [^{3}H]mazindol binding in the brain of amphetamine- and saline-treated WT and PTN-Tg mice in CPu, (C) in CPuM and (D) in CPuL. ** $p<0.01$ vs. Sal. *** $p<0.001$ vs. Sal. Abbreviations: CPu, Caudate putamen; CPuL, Lateral part of CPu; CPuM, Medial part of CPu.

Fig. 3. Amphetamine induces astrocytosis in the striatum of WT and PTN-Tg mice. (A) Photomicrographs are from GFAP-immunostained striatal sections of saline (Sal)- or amphetamine (Amph)-treated animals (n=4/group). Higher magnifications images in the lower right corner of every representative picture show that some of the astrocytes were hypertrophic and densely stained in WT mice treated with amphetamine whereas this effect

was generalized in PTN-Tg mice treated with amphetamine. (B) The graph represents quantification of data obtained from the counts of GFAP-positive cells in standardized areas of the striatum. *** P<0.001 vs. Sal. ### P<0.001 vs. WT-Amph. Scale bar 5x = 200 μm, 40x = 50 μm.

Fig. 4. [^{3}H] SCH23390 binding in WT and PTN-Tg mice treated with amphetamine. (A) Representative autoradiograms of [^{3}H] SCH23390 binding to D1 in the brain sections of WT and PTN-Tg mice treated with saline (Sal) or amphetamine (Amph) (n = 6/group). Representative autoradiograms of non-specific binding (NSB) was determined in adjacent sections in the presence of 10 μM cis-flupentixol. The colour bar represents pseudo-color interpretation of black and white film images in fmol/mg tissue. (B) Quantitative autoradiography of [^{3}H] SCH23390 binding in the brain of amphetamine- and saline-treated WT and PTN-Tg mice in CPu, (C) in CPuL and (D) in CPuM. Abbreviations: CPu, Caudate putamen; CPuL, Lateral part of CPu; CPuM, Medial part of CPu.

Fig. 5. [^{3}H]raclopride binding in WT and PTN-Tg mice treated with amphetamine. (A) Representative autoradiograms of [^{3}H]raclopride binding to D2 in the brain sections of WT and PTN-Tg mice treated with saline (Sal) or amphetamine (Amph) (n = 6/group). Representative autoradiograms of non-specific binding (NSB) was determined in adjacent sections in the presence of 10 μM sulpiride. The colour bar represents pseudo-color interpretation of black and white film images in fmol/mg tissue. (B) Quantitative autoradiography of [^{3}H]raclopride binding in the brain of amphetamine- and saline-treated WT and PTN-Tg mice in CPu, (C) in CPuL and (D) in CPuM. Abbreviations: CPu, Caudate putamen; CPuL, Lateral part of CPu; CPuM, Medial part of CPu.

Fig. 6. Amphetamine-induced conditioned place preference in PTN-Tg and WT mice. Preference score after amphetamine (3.0 mg/kg) conditioning, showing a significantly decreased amphetamine CPP in PTN-Tg mice. *P < 0.05 vs. WT.

Fig. 7. Schematic model of the effects of amphetamine in genetically engineered PTN mouse models. In normal WT mice, amphetamine (Amph) induces striatal denervation and an increase in the expression levels of PTN. PTN exerts neurotrophic actions on striatal dopaminergic terminals but also contribute to astrogliosis and cytokine release causing deleterious effects in the striatum. PTN-/- mice show an increased striatal denervation and a modest increase of astrogliosis, possibly caused by compensatory mechanisms triggered by factors downstream of PTN signaling pathways. PTN-Tg mice show an exacerbated striatal dopaminergic denervation after amphetamine treatment, together with a highly significant (4-fold) increase of astrogliosis which will overtake the possibly augmented neurotrophic effects caused by overexpression of PTN and will aggravate striatal dopaminergic injury.

	[^{3}H]SCH23390-specific binding (fmol/mg tissue)			
	Sal		Amph	
Region	WT	PTN-Tg	WT	PTN-Tg
Nucleus accumbens core	360.8 ± 40.3	369.2 ± 39.2	367.5 ± 43.7	362.8 ± 44
Nucleus accumbens shell	332 ± 44.1	346.8 ± 42.7	349.1 ± 37.4	339.7 ± 40
Olfatory tubercle	290 ± 26.4	285.9 ± 24.2	288.4 ± 31	299.4 ± 34.8
Clastrum	112.2 ± 19.3	99.8 ± 15	101.7 ± 15.3	95.4 ± 14.6
Cingulate cortex	26.9 ± 2.9	25.2 ± 2	24.8 ± 6.7	29 ± 4.4
Motor cortex	17.5 ± 2.5	19.4 ± 2.5	20 ± 3.9	20.8 ± 3.1
Amygdala	46.2 ± 6.9	49.6 ± 7.5	52.7 ± 6.7	47.2 ± 7.2
Thalamus	18.4 ± 2.9	24.3 ± 5.1	26.9 ± 5.6	26.1 ± 6.9
Hypothalamus	14.6 ± 3.5	21.5 ± 4.2	18.6 ± 3.3	21 ± 3.6
Hippocampus	26.2 ± 4	26.3 ± 6.6	38.5 ± 6.4	28.1 ± 6.1
Substantia nigra	184 ± 18.3	191.8 ± 10.8	204.1 ± 13.6	181 ± 10.2
Ventral tegmental area	21.3 ± 3.4	13.6 ± 2.9	18.6 ± 5.2	25.8 ± 8.2

Table 1. Quantitative autoradiography of [^{3}H]SCH23390 binding to D1 in brain sections of WT and PTN-Tg treated with amphetamine (Amph) or saline (Sal) (n = 6/group).

	[^{3}H]raclopride-specific binding (fmol/mg tissue)			
	Sal		Amph	
Region	**WT**	**PTN-Tg**	**WT**	**PTN-Tg**
Nucleus accumbens core	67.5 ± 11.8	54.2 ± 2.1	67.63 ± 11.8	60.6 ± 11.1
Nucleus accumbens shell	71.5 ± 12.5	70 ± 11.4	64.8 ± 11.4	69.3 ± 12.6
Olfatory tubercle	86.8 ± 16.5	76.6 ± 14.6	81.1 ± 15.6	82 ± 21.2

Table 2. Quantitative autoradiography of [^{3}H]raclopride binding to D2 in brain sections of WT and PTN-Tg treated with amphetamine (Amph) or saline (Sal) (n = 6/group).

Figure 1
Click here to download high resolution image

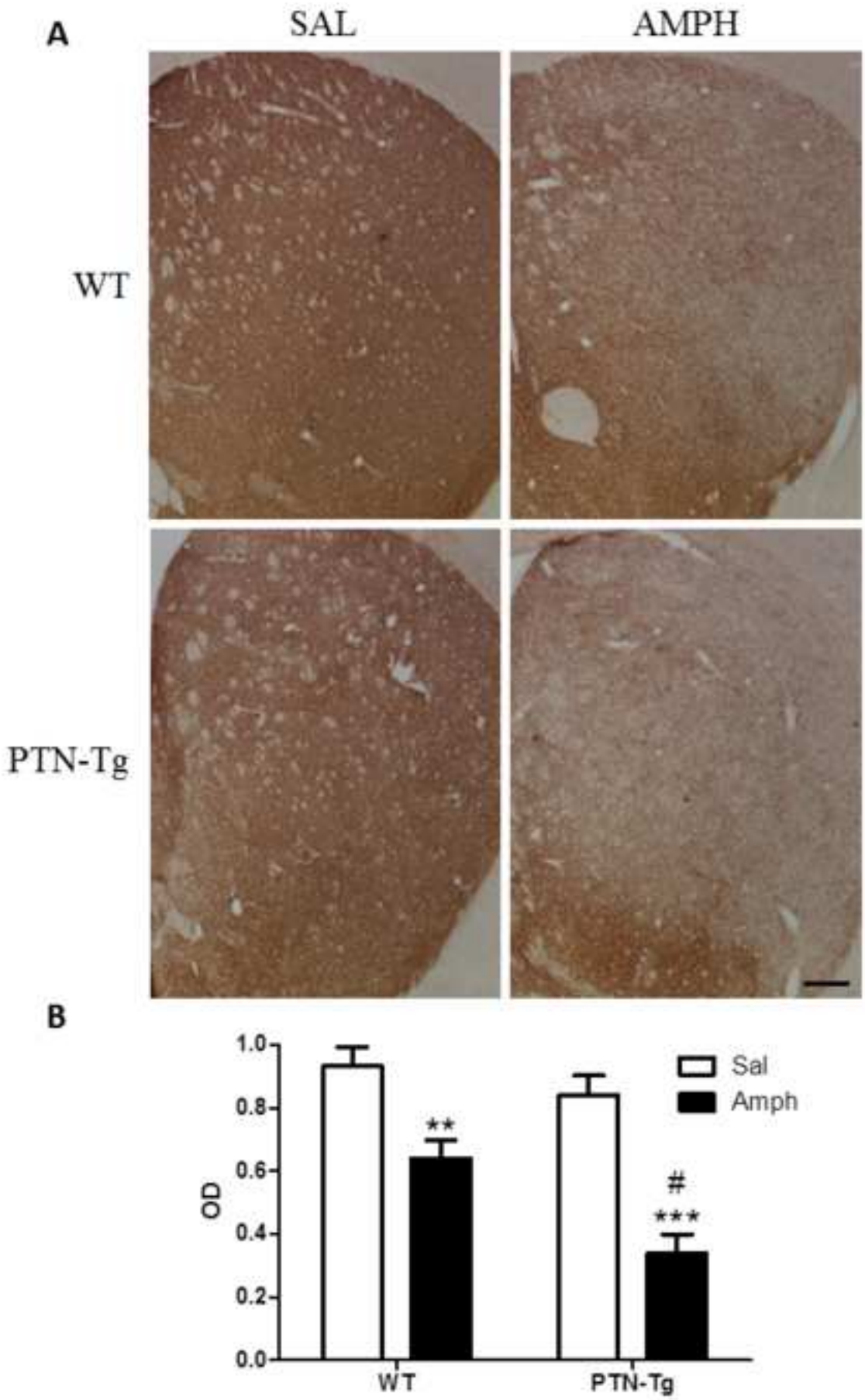

Fig. 1

Figure 2

Click here to download high resolution image

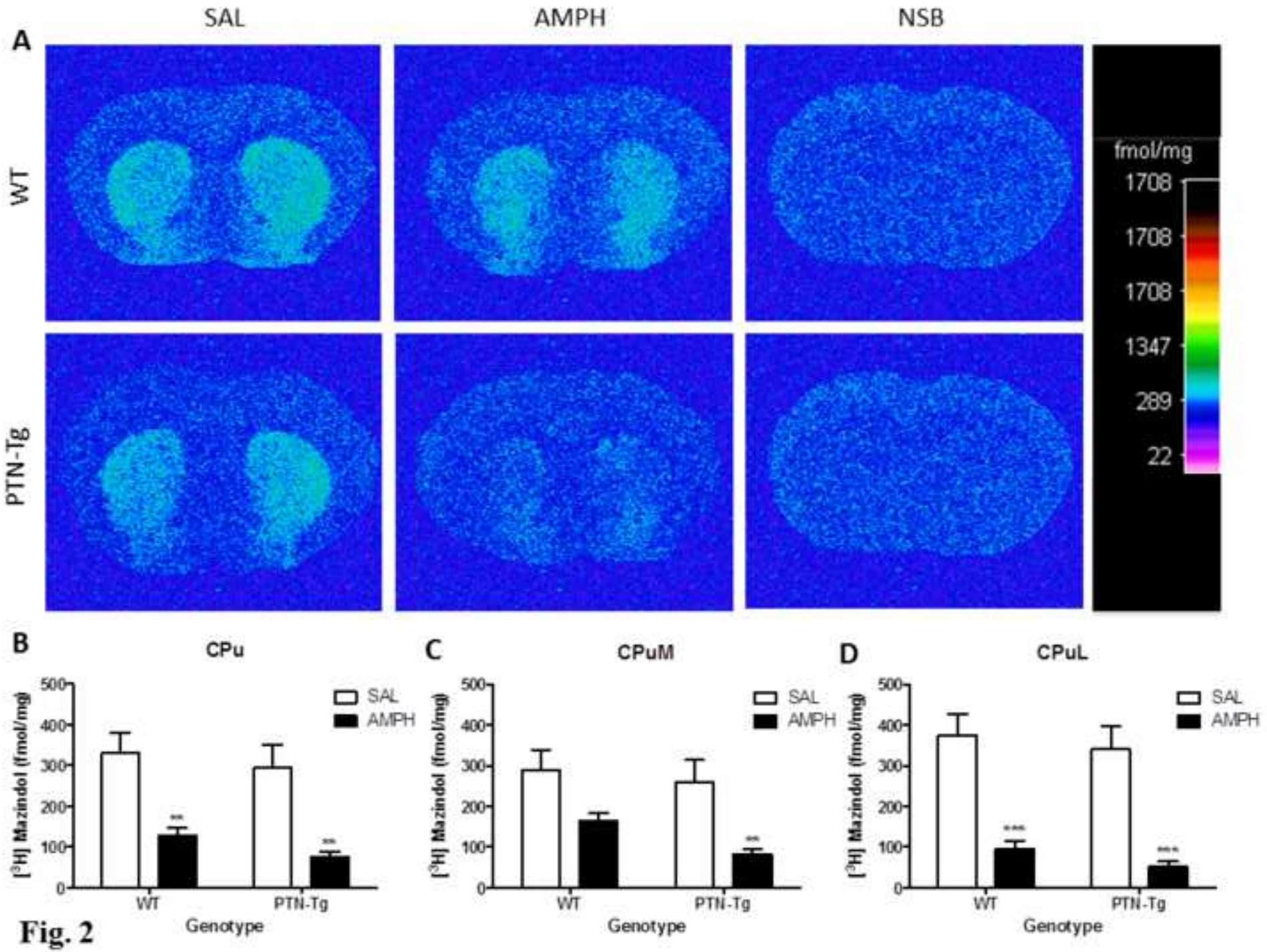

Fig. 2

Figure 3
Click here to download high resolution image

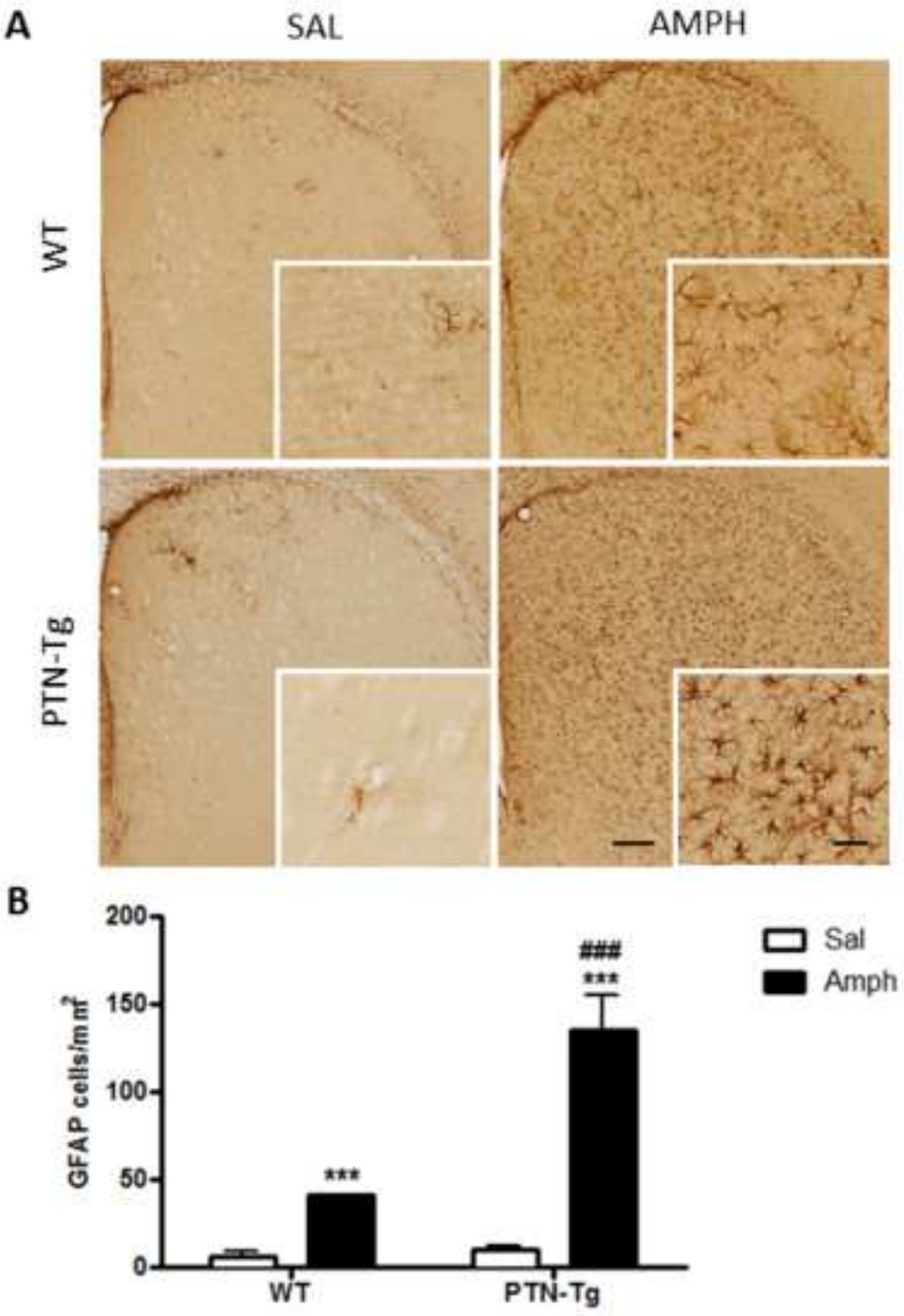

Fig. 3

Figure 4

Click here to download high resolution image

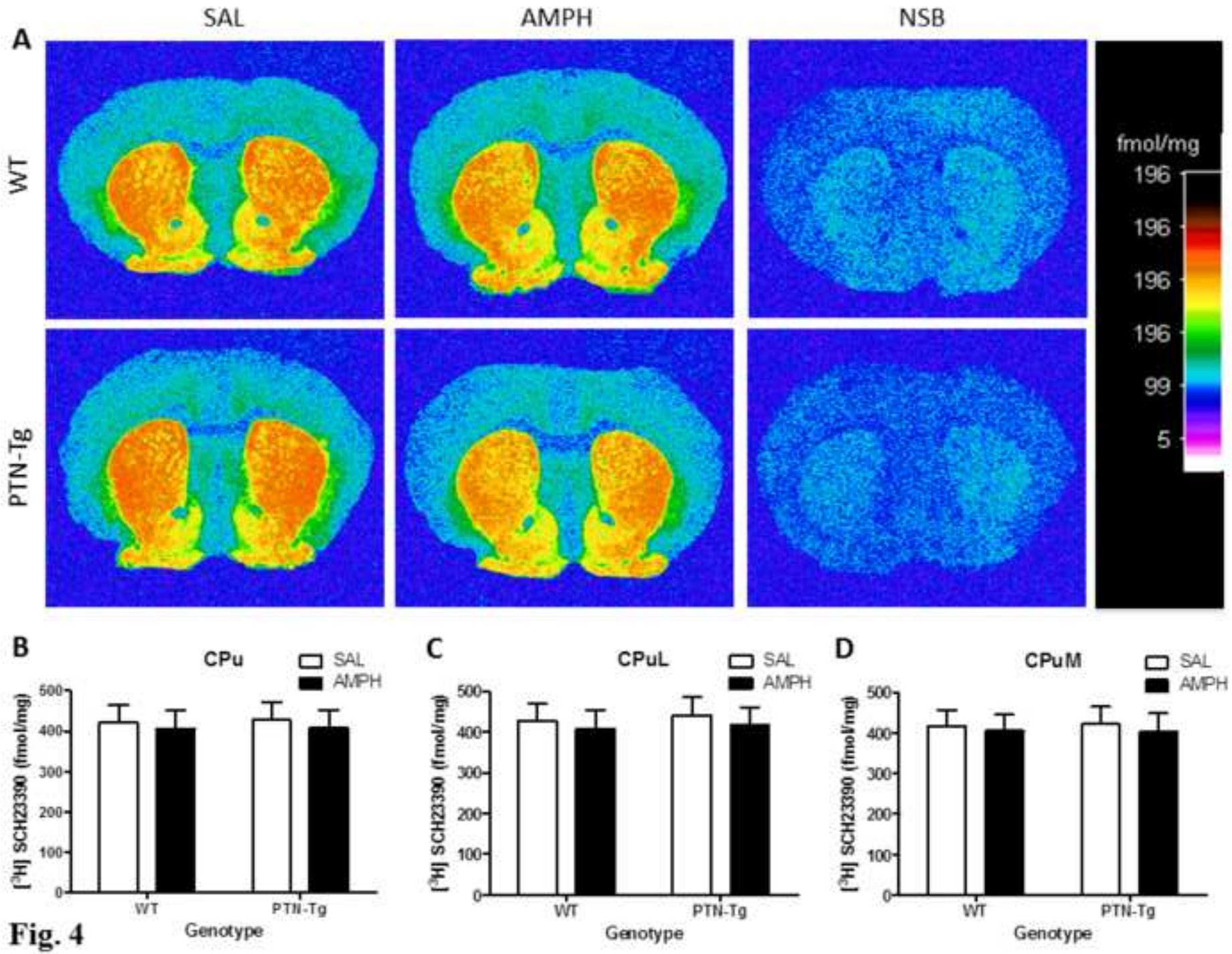

Fig. 4

Figure 5

Click here to download high resolution image

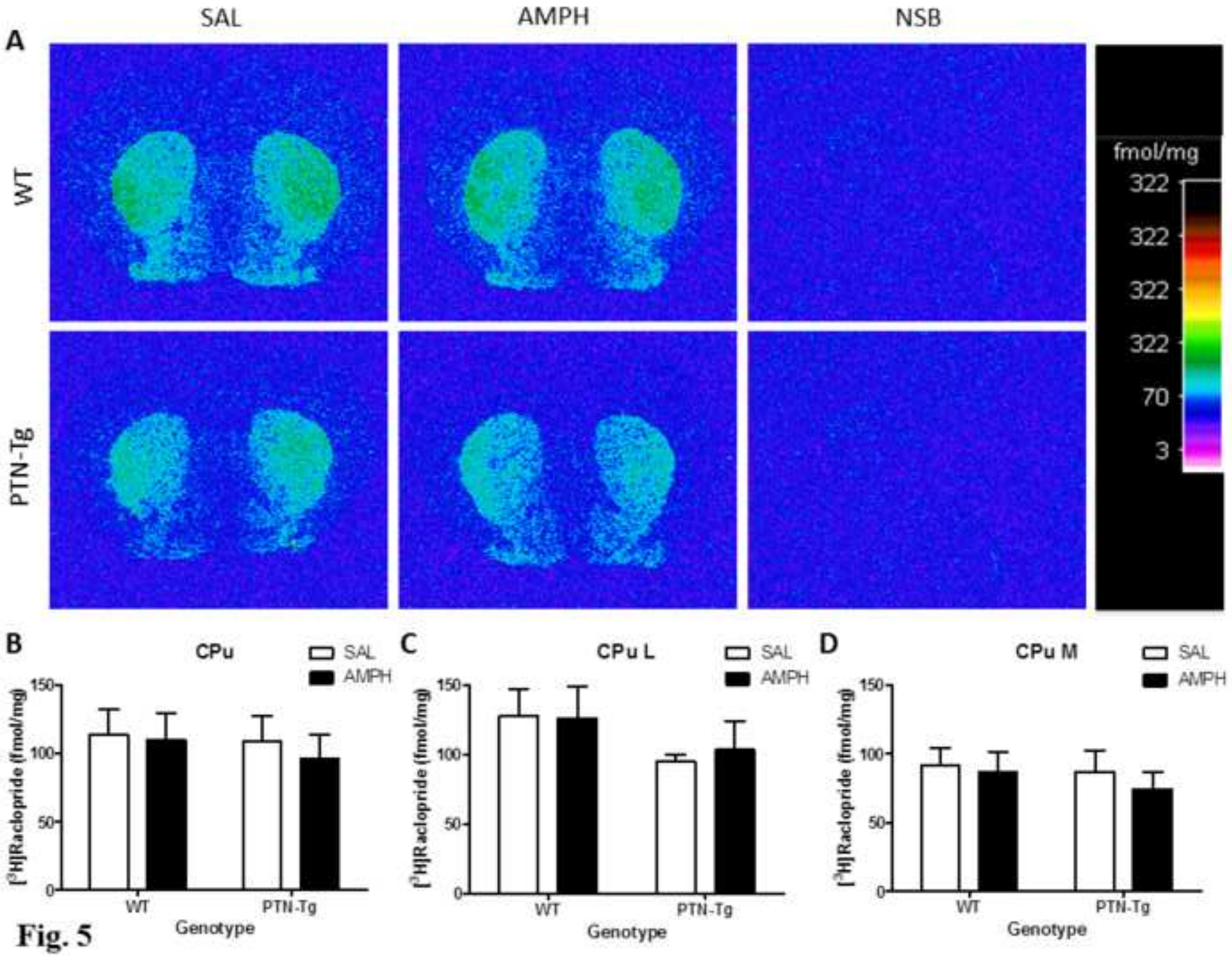

Fig. 5

Figure 6
Click here to download high resolution image

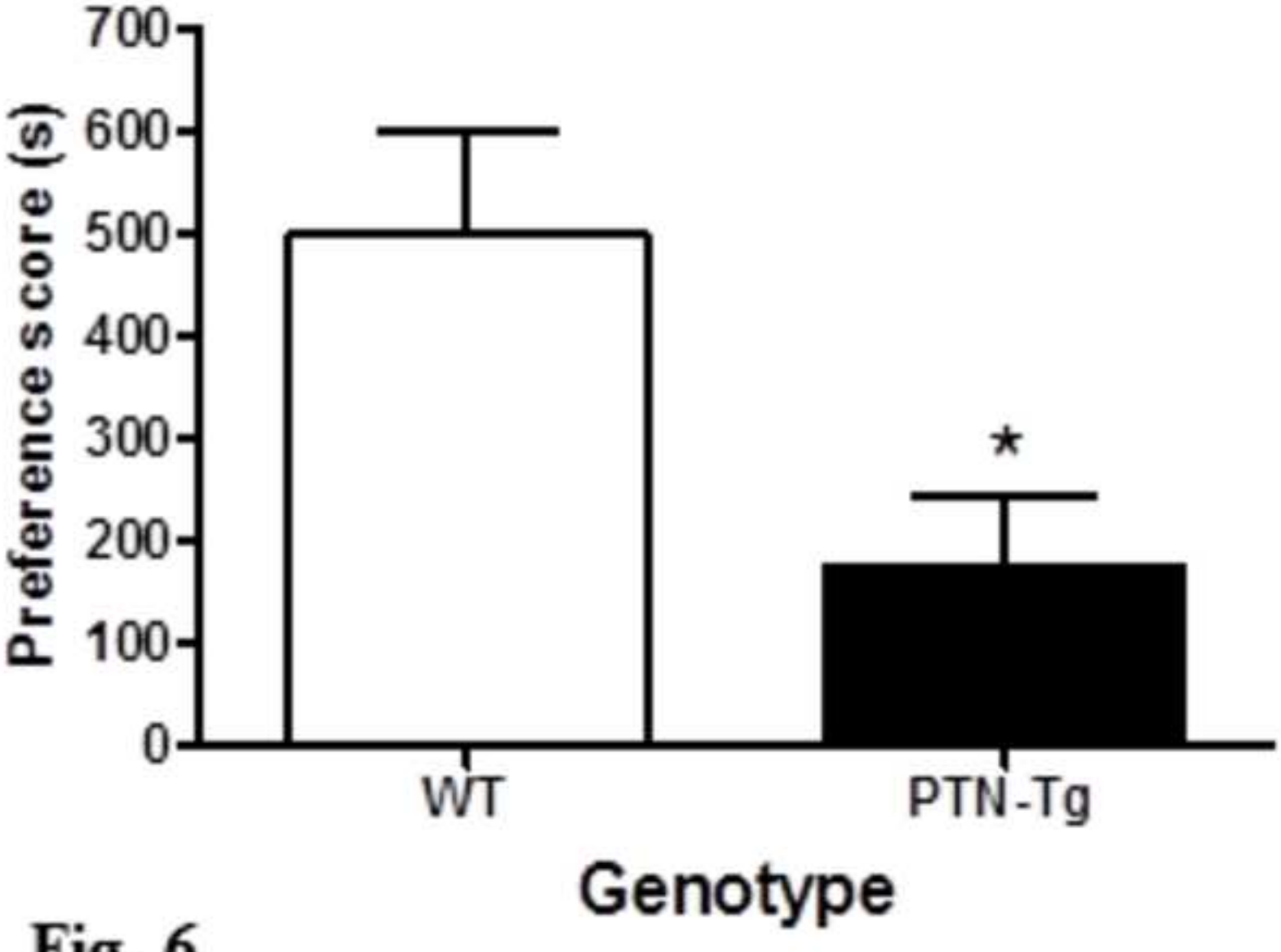

Fig. 6

Figure 7
Click here to download high resolution image

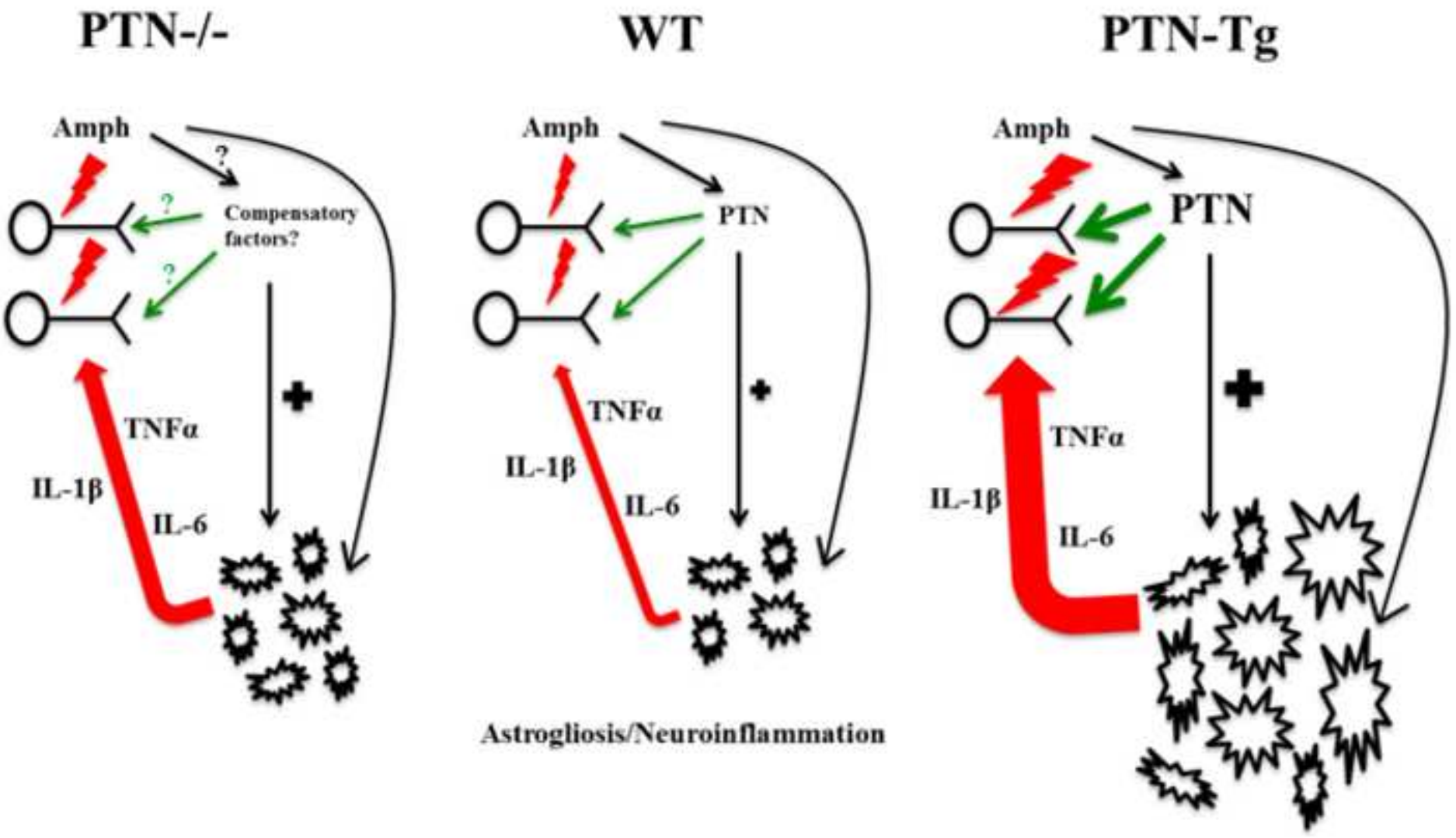

Fig. 7